NRC·CNRC

NRC Publications Archive
Archives des publications du CNRC

Time-of-flight spectroscopy with ultrafast all-optical gating

Fenwick, Kate L.; Thekkadath, Guillaume S.; Bustard, Philip J.; England, Duncan; Bouchard, Frédéric; Sussman, Benjamin

This publication could be one of several versions: author's original, accepted manuscript or the publisher's version. / La version de cette publication peut être l'une des suivantes : la version prépublication de l'auteur, la version acceptée du manuscrit ou la version de l'éditeur.

For the publisher's version, please access the DOI link below./ Pour consulter la version de l'éditeur, utilisez le lien DOI ci-dessous.

Publisher's version / Version de l'éditeur:

https://doi.org/10.1364/OE.549697

Optics Express, 33, 3, pp. 5914-5922, 2025-02-05

NRC Publications Archive Record / Notice des Archives des publications du CNRC :

https://nrc-publications.canada.ca/eng/view/object/?id=73e6c3d6-c14c-4bc6-81bc-239a17c3533e

https://publications-cnrc.canada.ca/fra/voir/objet/?id=73e6c3d6-c14c-4bc6-81bc-239a17c3533e

Access and use of this website and the material on it are subject to the Terms and Conditions set forth at https://nrc-publications.canada.ca/eng/copyright

READ THESE TERMS AND CONDITIONS CAREFULLY BEFORE USING THIS WEBSITE.

L'accès à ce site Web et l'utilisation de son contenu sont assujettis aux conditions présentées dans le site https://publications-cnrc.canada.ca/fra/droits

LISEZ CES CONDITIONS ATTENTIVEMENT AVANT D'UTILISER CE SITE WEB.

Questions? Contact the NRC Publications Archive team at PublicationsArchive-ArchivesPublications@nrc-cnrc.gc.ca. If you wish to email the authors directly, please see the first page of the publication for their contact information.

Vous avez des questions? Nous pouvons vous aider. Pour communiquer directement avec un auteur, consultez la première page de la revue dans laquelle son article a été publié afin de trouver ses coordonnées. Si vous n'arrivez pas à les repérer, communiquez avec nous à PublicationsArchive-ArchivesPublications@nrc-cnrc.gc.ca.

National Research Council Canada | Conseil national de recherches Canada

Canada

Research Article Vol. 33, No. 3 / 10 Feb 2025 / Optics Express 5914
Optics EXPRESS

Time-of-flight spectroscopy with ultrafast all-optical gating

KATE L. FENWICK,[1,2,*] GUILLAUME S. THEKKADATH,[2] PHILIP J. BUSTARD,[2] DUNCAN ENGLAND,[2] FRÉDÉRIC BOUCHARD,[2] AND BENJAMIN SUSSMAN[1,2]

[1]*Department of Physics, University of Ottawa, Advanced Research Complex, 25 Templeton Street, Ottawa ON Canada, K1N 6N5, Canada*
[2]*National Research Council of Canada, 100 Sussex Drive, Ottawa, Ontario K1A 0R6, Canada*
[*]*kfenw032@uottawa.ca*

Abstract: Spectral measurement is crucial in applications ranging from the investigation of matter and its electronic properties to the wavelength-multiplexed routing of optical signals. We propose and demonstrate a spectral measurement technique based on an all-optical approach. The signal spectrum is mapped to the time domain by dispersion in 1 km of fiber and is then optically gated by an intense ultrafast pulse in 10 cm of single-mode fiber. A portion of the signal spectrum can be recovered by sweeping the gate pulse through the stretched signal. Spectral fringes are measured down to the minimum bound for frequency-to-time mapping of 51.5 GHz. Our measurement technique expands the toolbox of ultrafast measurements from the time domain to the frequency domain.

© 2025 Optica Publishing Group under the terms of the Optica Open Access Publishing Agreement

1. Introduction

Spectral measurement of light is one of the most fundamental exploratory tools in astronomy [1], chemistry [2], and physics [3]. Measuring the spectrum resulting from light-matter interactions provides information on the composition and structure of matter, from atomic [4] to astronomical [5] scales. Not only is spectral measurement crucial for understanding material properties, it is also important for characterizing optical signals, such as ultrafast pulses [6,7] or single photons [8,9]. In many cases, high spectral resolution is required, for example when characterizing optical frequency combs [10] or spectral fringes [11,12], or in optical communication where different wavelengths of light can be used to send multiple signals at once over a fiber optic communication channel (*i.e.,* wavelength-division multiplexing) [13]. Frequency-to-space mapping in a grating spectrometer is perhaps the most common method used for spectral measurement; however, numerous techniques exist. Some techniques do not even require direct measurement in the frequency-domain, allowing for high-resolution capabilities in other domains (*e.g.,* time) to be exploited, as we demonstrate here.

Fourier transform spectroscopy, for example, measures interference in the time-domain to build optical spectrograms [14]. Another time-domain implementation, which has attracted attention in the last decade, is time-of-flight spectroscopy [15,16]. This technique uses time-domain "diffraction", where a highly dispersive medium maps the spectrum of an input ultrafast pulse to the temporal envelope of its output [17–19]. The stretched pulse is then measured by a high-speed photodetector, where the time-dependent intensity informs the spectrum [20–22]. At the single-photon level, frequency-to-time mapping has been implemented with dispersion compensating fiber [9] and chirped fiber Bragg gratings [8] to measure the spectra of single photons. Time-stretched single-photon spectra are monitored by fast single-photon counting modules, which demonstrates the potential for real-time measurement of multiple bits of information per single photon. Recent advancements in single-photon detection have led to increasingly precise timing

#549697 https://doi.org/10.1364/OE.549697
Journal © 2025 Received 3 Dec 2024; revised 10 Jan 2025; accepted 24 Jan 2025; published 5 Feb 2025

Optics EXPRESS

resolution and fewer dark counts. Superconducting nanowire single-photon detectors (SNSPDs) routinely achieve timing resolution around 100 ps, with cutting-edge systems reaching down to the sub-10 ps timescale [23,24]; but there is always room for improvement.

In particular, when detection bandwidth is limiting the resolution of a time-of-flight spectrometer, one might consider using nonlinear optical gating [7] to reach detection bandwidths beyond what can be achieved electronically [25]. Importantly, the gating should not introduce a prohibitive amount of noise in the signal, especially when this is a single photon [26]. Low-noise gating based on linear interferometric techniques can be used to overcome detection bandwidth limitations [27–31]. Nonlinear techniques can operate without the need for an interferometer, and have been demonstrated using upconversion as the gating mechanism [32], but this method inherently requires a frequency conversion and is limited in terms of efficiency. Another promising all-optical approach–which has already demonstrated broad applicability in ultrafast pulse shaping [33], characterization of energy-time entangled photons [34], quantum communications [35], quantum simulations [36], and quantum information processing [37]–uses optical Kerr gating. By extending this optical Kerr gating technique to the spectral domain via frequency-to-time mapping, we anticipate a scheme that could pave the way for new advancements in spectral characterization and manipulation.

Here, we propose and demonstrate a spectral measurement technique that uses ultrafast optical Kerr gating of a frequency-to-time mapped signal. Outlined in Fig. 1, group velocity dispersion (GVD) in 1 km of fiber is used to stretch an input signal pulse, effectively mapping its spectrum to the time-domain. This time-stretched signal is then gated by an ultrafast pump pulse through the optical Kerr effect in 10 cm of single-mode fiber (SMF), depicted in the inset of Fig. 1. The pump pulse overlaps with a narrow window of the stretched signal pulse in time, and thus also a

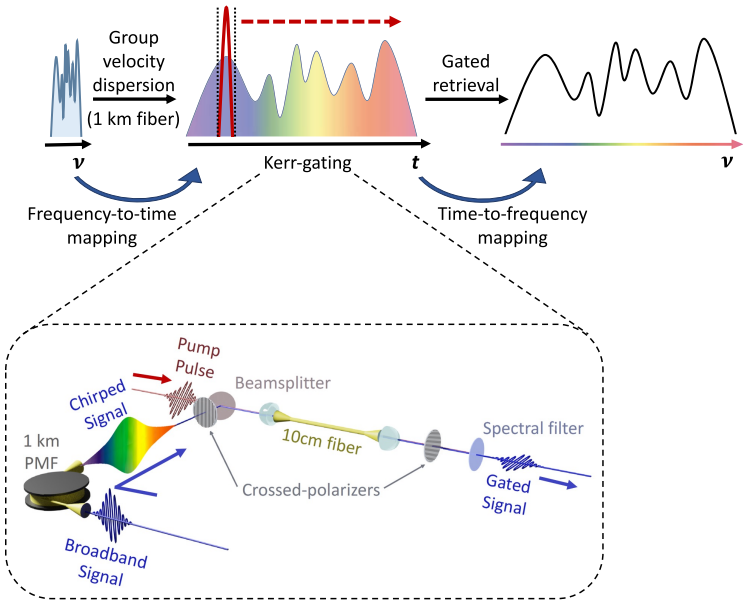

Fig. 1. Operating principle for Kerr-gated spectral measurement. A dispersive medium (such as a long optical fiber) is used to stretch an optical signal of interest and thus map its spectrum to the time-domain. Kerr-gating, shown in the inset, uses an intense ultrafast pump pulse to rotate the polarization of a narrow temporal window in the dispersed signal pulse. The gated signal is measured for various delay between signal and pump, and can be used to retrieve the optical spectrum.

Optics EXPRESS

narrow frequency band. This induces polarization rotation in the signal within the window of overlap. When the SMF is placed between two crossed-polarizers, only the polarization-rotated signal is transmitted, thus sampling a narrow frequency band for detection. This technique offers tunability in its operating band and the potential for full fiber-integration.

2. Theoretical requirements

We first consider the requirements of implementing frequency-to-time mapping. The output field, $E_{\text{out}}(t)$, for a pulse propagating through group delay dispersion, $\beta_2 z$ (where z is the length of the dispersive medium with quadratic dispersion β_2), is given by the convolution of the input field, $E_{\text{in}}(t)$, with a quadratic phase function: $E_{\text{out}} \sim E_{\text{in}} * \mathrm{e}^{it^2/2\beta_2 z}$ (see Supplement 1 for more details); this result is isomorphic with that for Fresnel diffraction in one dimension. In analogy to the spatial domain, the longest temporal feature duration of the input pulse, τ_0, determines the dispersion required to be in the "far field", where each spectral component is mapped to a different time in the output pulse. This condition is met when $|\beta_2 z| \gg \tau_0^2/8$, in which case the time-stretched output pulse is a scaled version of its input spectrum:

$$E_{\text{out}}(t) = \sqrt{\frac{-i}{2\pi\beta_2 z}}\, \mathrm{e}^{it^2/2\beta_2 z}\, \mathrm{e}^{i\omega_0 t} \widetilde{E}_{\text{in}}(\omega = \omega_0 + \frac{t}{\beta_2 z}), \tag{1}$$

where angular frequency is given by $\omega = 2\pi f$ and $\omega_0 = 2\pi f_0$ is the carrier frequency of the pulse. Frequency, f, is thus mapped on to time with a mapping factor of [38],

$$2\pi \frac{\partial f}{\partial t} = \frac{1}{\beta_2 z}. \tag{2}$$

Given that the finest spectral feature, δf, and its duration are related by the time-bandwidth product, $\tau_0\, \delta f \sim 1$, in order to obtain an accurate spectrum, the finest spectral feature, δf, must satisfy [38]

$$\delta f \gg \frac{1}{\sqrt{8|\beta_2 z|}}. \tag{3}$$

We can use this to estimate a minimum bound, δf_{min}, for frequency-to-time mapping with a given group delay dispersion,

$$\delta f_{\text{min}} = \frac{1}{\sqrt{8|\beta_2 z|}}, \tag{4}$$

with the understanding that spectral distortions will increase as δf_{min} is approached. In many cases, the spectral measurement resolution will be limited by the detector timing resolution. For a detector with timing resolution, $\Delta\tau_D$, the corresponding frequency bandwidth is given by

$$\Delta f_D = \frac{\Delta\tau_D}{2\pi|\beta_2 z|}. \tag{5}$$

It is commonly appreciated that the resolution of the frequency-to-time mapping technique is determined by the ratio of the detector (or gate) speed to the dispersion; however, care must be taken to ensure that Eq. (3) is satisfied, or the measured trace will include distortions. In order to accurately reconstruct the spectrum for a given dispersion, $\Delta f_D \lesssim \delta f_{\text{min}}$ should be met, placing a limit on the necessary detector resolution. For more details on the theory of frequency-to-time mapping, see Supplement 1.

Optics EXPRESS

3. Experimental implementation

The experimental setup for the Kerr-gate frequency sampler is shown in Fig. 2. Both the signal and pump originate from an 80 MHz titanium sapphire (Ti:Sapph) laser, centered at 816 nm with a spectral bandwidth of 12 nm. The output pulses are split into two paths by a half-wave plate ($\lambda/2$) and polarizing beam splitter (PBS), which are used to control the pulse energy in the signal (reflected) path. The pulse energy in the pump (transmitted) path is controlled by a second $\lambda/2$ wave plate and PBS combination. Supercontinuum generation (SCG) in a 12 cm photonic crystal fiber (PCF) provides a signal pulse in a different spectral region than the pump, which is a requirement for operating the Kerr gate. The broadband light generated in the PCF is shown in Fig. 2(a). Pump pulses with energy ~ 0.055 nJ are used to generate the spectrum shown in blue, which is then spectrally filtered using a 5 nm bandpass filter (shown in red).

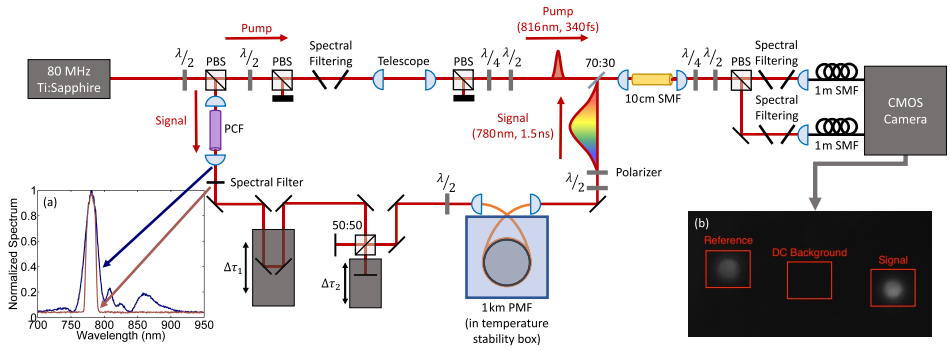

Fig. 2. Experimental setup. An 80 MHz Ti:Sapphire oscillator is split along two paths by a half-wave plate ($\lambda/2$) and polarizing beam splitter (PBS). The signal provides the spectrum to be gated, and the pump does the gating. Supercontinuum generation in a photonic crystal fiber (PCF) provides broadband signal light, depicted in (a), which is delayed with respect to the pump, $\Delta\tau_1$. A Michelson interferometer is used to prepare two signal pulses delayed by $\Delta\tau_2$, providing spectral fringes for measurement. 1 km of polarization maintaining fiber (PMF), housed in a temperature-stability box, provides the frequency-to-time mapping of the signal. The $\lambda/2$ wave plate prior to the 1 km PMF rotates the signal polarization such that it is aligned to the slow axis of the PMF. The time-stretched signal polarization is prepared by a $\lambda/2$ wave plate and absorptive polarizer. The pump polarization is prepared by a polarizing beam splitter (PBS) and a quarter- ($\lambda/4$) and half- ($\lambda/2$) wave plate. The pump and signal are recombined by a 70:30 (70% reflection, 30% transmission) beam splitter, and are then coupled into the 10 cm single mode fiber (SMF) for Kerr-gating. Only polarization-rotated light is allowed through the $\lambda/2$, $\lambda/4$, PBS combination after the SMF, to be measured by a CMOS camera. Shown in (b), the rejected light is also monitored on the CMOS camera, and allows for common-mode noise division where applicable.

The signal light is then sent through a variable delay line, $\Delta\tau_1$, to allow the control of the relative delay between the signal pulse and pump pulse. We use a Michelson interferometer with tunable delay $\Delta\tau_2$ between the two arms to impart a controllable spectral signature onto the signal. Pulses exiting the interferometer exhibit spectral fringes with frequency $f = 1/\Delta\tau_2$ [6,39]. After this, 1 km of polarization-maintaining fiber (PMF) disperses the signal pulses, with dispersion parameter $D = -146.1$ ps/nm/km (corresponding to quadratic dispersion $\beta_2 = 47.2$ ps^2/km). The signal pulse energy prior to the 1 km PMF is 690 fJ. Signal pulse propagation time in the 1 km fiber can drift due to thermal expansion of the glass. Based on the range of values for the thermal expansion coefficient of optical glass [40], the signal pulse arrival time drift is expected to be between $\approx 13 - 53$ ps/K. To slow this drift, the 1 km PMF is housed in a temperature-stable box. Note that the $\lambda/2$ wave plate prior to the PMF is used to rotate the signal polarization such that it

Optics EXPRESS

couples to the slow axis of the PMF. After the PMF, the polarization of the time-stretched signal is then prepared by a $\lambda/2$ wave plate and nanoparticle polarizer, and recombined with the pump on a 70:30 beam splitter (70% of the signal is reflected, 30% of the pump is transmitted).

The stretched signal is then gated by the pump pulse within the 10 cm SMF (Thorlabs S630-HP). As outlined in Supplement 1, it is important that the pump polarization is at 45° relative to the signal polarization for Kerr gating. The pump polarization is set by a PBS, quarter- ($\lambda/4$) wave plate, and $\lambda/2$ wave plate. The portion of the signal that is overlapped temporally with the pump will experience polarization rotation due to the Kerr effect. A PBS at the output of the 10 cm SMF allows only polarization-rotated light through to the detector. It is preceded by $\lambda/4$ and $\lambda/2$ wave plates, which compensate for any intrinsic birefringence within the 10 cm SMF. After the PBS, spectral filters are used to attenuate the pump, and a 1 m SMF is used to spatially filter any light allowed to propagate in the cladding modes of the short 10 cm SMF. The polarization rotated light (signal) is measured using a CMOS camera (Thorlabs, DCC1645C). The light reflected at the PBS can be measured simultaneously on the CMOS camera (reference), allowing for common-mode noise division, if desired. Note that, for the data presented here, we perform a background subtraction rather than make use of the common-mode noise division option; however, we include the option of measuring the reference signal in Fig. 2 for completeness. For our background subtraction, we take measurements of the Kerr gated signal (both pump and signal on) and subtract the background noise due to the pump (pump on, signal blocked). The integrated DC background should be subtracted from both the integrated signal and reference spots on the camera in all cases.

The Kerr gate pump pulse can introduce noise photons in the signal spectral band due to competing parasitic nonlinear processes such as fluorescence, Raman scattering, self-phase modulation (SPM), and two-photon fluorescence [41], especially when the pump and signal are in similar spectral regions. We mitigate these noise sources by spectrally filtering the pump prior to Kerr gating and also reducing its power, the latter of which limits our gating efficiency to $\sim$ 30%. However, previous works have shown that the Kerr gate can reach near-unit efficiencies with low noise, when the signal and pump center wavelengths are well-separated [35,42].

4. Results and discussion

The setup was first operated without the Michelson interferometer to measure the dispersion parameter in the 1 km PMF. Instead of the CMOS camera, an Ocean Optics USB2000+ spectrometer was used to measure the spectrum of the gated signal. When the stretched signal is delayed relative to the gate (pump) pulse, the gate overlaps with different signal frequencies. As expected, this causes the central wavelength of the gated signal to shift with gate pulse delay. This is shown in Fig. 3, where the slope of a linear fit allows for the experimental measurement of the dispersion parameter in the 1 km PMF. The experimental dispersion parameter was measured to be -146.1 ± 0.4 ps/nm (for $\sim$ 1 km of fiber), which is close to the quoted dispersion parameter from Thorlabs of -150 ps/nm/km at 780 nm. With a measurement of dispersion, time (Kerr-gate delay $\Delta\tau_1$) can be mapped to frequency. For this amount of dispersion, the minimum bound for frequency-to-time mapping is $\delta f_{\text{min}} = 51.5$ GHz, which corresponds to a required detector speed of 15.2 ps. Interestingly, since we operate with a sub-picosecond Kerr gate resolution, we are limited here by the amount of dispersion rather than the speed of our detection mechanism.

With the Michelson interferometer in the experimental setup, spectral fringes can be measured with the Kerr gate. By increasing the signal pulse separation, we can generate increasingly narrow spectral features down to the minimum bound for frequency-to-time mapping; for $\delta f_{\text{min}} = 51.5$ GHz, this is given by $\Delta\tau_2 = 19.5$ ps. Figures 4(a)–(f) compare measured fringes with a model for pulse separation within the frequency-to-time mapping regime, while Fig. 4(g) presents the same comparison just beyond the limit of Eq. (4). The model follows the theory of frequency-to-time mapping presented in Supplement 1, where the input signal is taken to be two

Optics EXPRESS

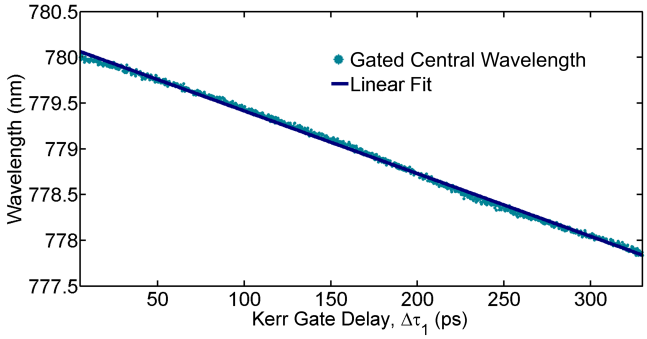

Fig. 3. Measuring the dispersion parameter. Central wavelength of polarization-rotated light is plotted against Kerr-gate delay (light blue). Over the small range of wavelengths measured, a linear fit (dark blue) can be used to extract the dispersion parameter of the 1 km fiber: -146.1 ± 0.4 ps/nm.

100 fs Gaussian pulses separated by a time delay of $\Delta\tau_2$. Note that $\Delta\tau_2$ is estimated based on the measured fringe spacing to account for any stage misalignment relative to the optical axis. The modeled temporal profile of the input signal is then converted to the frequency domain by a fast Fourier transform (FFT), after which a quadratic phase operator, associated with dispersion in the 1 km PMF, is multiplied. The result is then converted back to the time domain by inverse fast Fourier transform (IFFT), and a cross-correlation with the Kerr gate intensity profile (for $\lambda_{\text{signal}} = 780$ nm, $\lambda_{\text{pump}} = 816$ nm, and a pump pulse with 340 fs duration and energy of 0.69 nJ) is performed. This end result can then be compared with experimental measurements, as presented in Fig. 4. We observe good qualitative agreement between our experimental data and model.

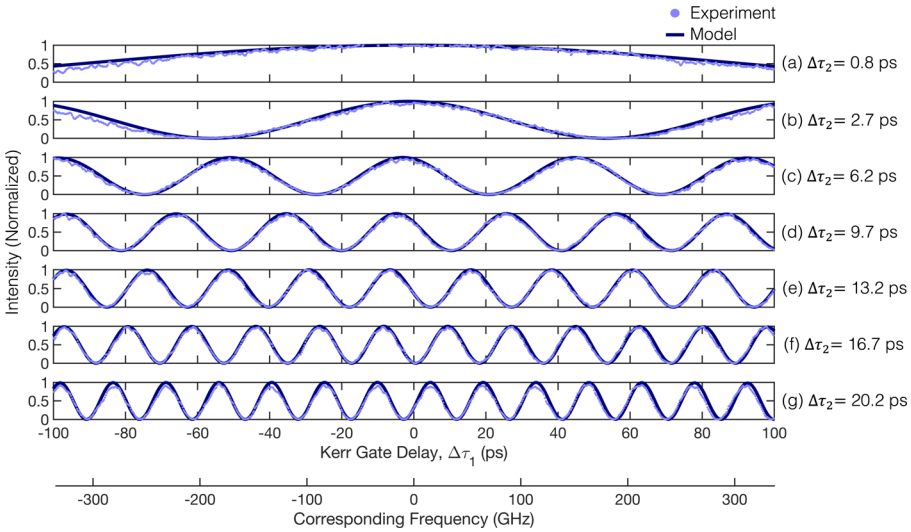

Fig. 4. Spectral fringes within and near the frequency-to-time mapping limit. Measured fringes (light purple) are compared with modeled fringes (dark blue) for various signal pulse delay, $\Delta\tau_2$. The respective frequency axis, calculated using Eq. (2), is displayed at the bottom for reference. Note that the data presented in (g) has spectral features smaller than the limit in Eq. (4), and is thus outside the frequency-to-time mapping regime.

Optics EXPRESS

The full measurement window is limited by the scanning range of the motorized delay line, $\Delta\tau_1$. Here, we are limited to a measurement spanning 200 ps, and thus only measure a portion of the signal spectrum; however, this window can be increased with the use of larger motorized linear delay stages. The acquisition time of a single data point (*i.e.,* the intensity of a Kerr-gated spectral component of the signal) is approximately 360 ms. Since we perform a measurement of both the gated signal (pump and signal on) and background noise due to the pump (pump on, signal off), the total acquisition time required for each spectrum presented in Fig. 4 takes about 9 minutes (2×4.5 minutes, to acquire both a signal and background). This total scan duration can be optimized to suit experimental needs, by adjusting the detector integration time and scanning resolution.

5. Conclusions and outlook

In summary, we have demonstrated a technique for time-of-flight spectroscopy using ultrafast optical Kerr gating. The spectrum of interest is first mapped to the time-domain by applying dispersion, after which an optically gated measurement is performed. Spectral fringes are measured down to the minimum bound for frequency-to-time mapping, with good agreement observed between experiment and model. Although time-of-flight spectroscopy is often limited by detector timing resolution, we stress the importance of recognizing that this is not always the case. Here, the detection resolution surpasses that of the minimum bound set by dispersion.

The high speed of ultrafast optical Kerr gating in fiber, combined with its potential for high-efficiency and low-noise operation [35,43], make this an attractive technique for operating on broadband single-photon-level signals. Indeed, optical Kerr gating has already seen application in fields such as time-resolved fluorescence emission spectroscopy [44–48], where spectral measurement of fluorescence can be performed without frequency-to-time mapping. Here, we explored the possibility of Kerr-gated measurement in the spectral domain, down to the estimated minimum resolution bound for frequency-to-time mapping, $\delta f_{\text{min}} = 51.5$ GHz. For comparison, state-of-the-art time-of-flight spectrometers have seen approximately 213 GHz resolution in the 4.4–4.9 μm range [22], 90 GHz resolution at 1550 nm [9] 24 GHz resolution at 830 nm [8], and an impressive 1.9 GHz resolution around 1550 nm [21]. We anticipate that, with increased dispersion, the optical Kerr gate will be capable of higher-resolution measurement, competitive with state-of-the-art demonstrations. Obtaining sufficient dispersion to complement the high speed of the Kerr gate is a challenge; the temporal duration corresponding to the minimum frequency bound will also increase with dispersion. Furthermore, propagation in long fiber requires temperature stabilization. Chirped fiber Bragg gratings could provide one avenue for achieving higher group delay dispersion without the need for temperature stabilization; however, in this case, one must consider the trade-off between increased dispersion and loss. It is also important to weigh the time cost of performing a scanning measurement against the potential resolution benefits of the high-speed Kerr gate.

Nevertheless, intriguing possibilities remain: this technique could enable selective modulation or re-routing of optical signals based on frequency, for example, in frequency demultiplexing or for the manipulation of frequency-bins in quantum information processing schemes. With the implementation of multiple Kerr gates, frequency demultiplexing could be performed with minimal scanning. One may also envision combining time-bin and frequency-bin encoding in quantum information processing through this technique. Our approach could also be generalized to encompass spectro-temporal measurements; by adjusting the dispersion applied, one could apply selective phase and amplitude modulations to spectro-temporal modes. One could also explore the use of tomographic techniques [49] to better estimate the signal spectrum when the measurement resolution is limited by dispersion.

Funding. Natural Sciences and Engineering Research Council of Canada; Vanier Canada Graduate Scholarships (Vanier CGS) program.

Optics EXPRESS

Acknowledgments. We thank Aaron Goldberg, Alicia Sit, Andrew Proppe, Brayden Freitas, Denis Guay, Doug Moffatt, Kent Bonsma-Fisher, Khabat Heshami, Milica Banic, Nicholas Couture, Noah Lupu-Gladstein, Ramy Tannous, Rune Lausten, and Yingwen Zhang for their support and insightful discussions.

Disclosures. The authors declare no conflicts of interest.

Data availability. Data underlying the results presented in this paper are not publicly available at this time but may be obtained from the authors upon reasonable request.

Supplemental document. See Supplement 1 for supporting content.

References

1. J. B. Hearnshaw, *The analysis of starlight: one hundred and fifty years of astronomical spectroscopy* (CUP Archive, 1990).
2. J. Ingle and S. Crouch, *Prentice–Hall/Englewood Cliffs* (CUP Archive, 1988).
3. S. Dattagupta, *Relaxation phenomena in condensed matter physics* (Elsevier, 2012).
4. J. Stewart, J. Gaebler, and D. Jin, "Using photoemission spectroscopy to probe a strongly interacting Fermi gas," Nature **454**(7205), 744–747 (2008).
5. J. Angel, A. Cheng, and N. Woolf, "A space telescope for infrared spectroscopy of Earth-like planets," Nature **322**(6077), 341–343 (1986).
6. C. Iaconis and I. A. Walmsley, "Self-referencing spectral interferometry for measuring ultrashort optical pulses," IEEE J. Quantum Electron. **35**(4), 501–509 (1999).
7. D. J. Kane and R. Trebino, "Characterization of arbitrary femtosecond pulses using frequency-resolved optical gating," IEEE J. Quantum Electron. **29**(2), 571–579 (1993).
8. A. O. Davis, P. M. Saulnier, M. Karpiński, *et al.*, "Pulsed single-photon spectrometer by frequency-to-time mapping using chirped fiber bragg gratings," Opt. Express **25**(11), 12804–12811 (2017).
9. M. Avenhaus, A. Eckstein, P. J. Mosley, *et al.*, "Fiber-assisted single-photon spectrograph," Opt. Lett. **34**(18), 2873–2875 (2009).
10. A. Schliesser, N. Picqué, and T. W. Hänsch, "Mid-infrared frequency combs," Nat. Photonics **6**(7), 440–449 (2012).
11. J. Morgenweg, I. Barmes, and K. S. Eikema, "Ramsey-comb spectroscopy with intense ultrashort laser pulses," Nat. Phys. **10**(1), 30–33 (2014).
12. L. Dreissen, C. Roth, E. Gründeman, *et al.*, "High-precision Ramsey-comb spectroscopy based on high-harmonic generation," Phys. Rev. Lett. **123**(14), 143001 (2019).
13. A. Sharkawy, S. Shi, and D. W. Prather, "Multichannel wavelength division multiplexing with photonic crystals," Appl. Opt. **40**(14), 2247–2252 (2001).
14. F. Adler, P. Masłowski, A. Foltynowicz, *et al.*, "Mid-infrared Fourier transform spectroscopy with a broadband frequency comb," Opt. Express **18**(21), 21861–21872 (2010).
15. J. Chou, Y. Han, and B. Jalali, "Time-wavelength spectroscopy for chemical sensing," IEEE Photonics Technol. Lett. **16**(4), 1140–1142 (2004).
16. D. Solli, J. Chou, and B. Jalali, "Amplified wavelength–time transformation for real-time spectroscopy," Nat. Photonics **2**(1), 48–51 (2008).
17. Y. Tong, L. Chan, and H. Tsang, "Fibre dispersion or pulse spectrum measurement using a sampling oscilloscope," Electron. Lett. **33**(11), 983–985 (1997).
18. V. Torres-Company, J. Lancis, and P. Andres, "Space-time analogies in optics," Prog. Opt. **56**, 1–80 (2011).
19. K. Goda and B. Jalali, "Dispersive Fourier transformation for fast continuous single-shot measurements," Nat. Photonics **7**(2), 102–112 (2013).
20. A. Mahjoubfar, D. V. Churkin, S. Barland, *et al.*, "Time stretch and its applications," Nat. Photonics **11**(6), 341–351 (2017).
21. J. Mance, B. La Lone, J. Madajian, *et al.*, "Time-stretch spectroscopy for fast infrared absorption spectra of acetylene and hydroxyl radicals during combustion," Opt. Express **28**(20), 29004–29015 (2020).
22. A. Kawai, K. Hashimoto, T. Dougakiuchi, *et al.*, "Time-stretch infrared spectroscopy," Commun. Phys. **3**(1), 152 (2020).
23. I. E. Zadeh, J. W. Los, R. B. Gourgues, *et al.*, "Efficient single-photon detection with 7.7 ps time resolution for photon-correlation measurements," ACS Photonics **7**(7), 1780–1787 (2020).
24. B. Korzh, Q.-Y. Zhao, J. P. Allmaras, *et al.*, "Demonstration of sub-3 ps temporal resolution with a superconducting nanowire single-photon detector," Nat. Photonics **14**(4), 250–255 (2020).
25. B. Crockett, C. M. Rowe, and J. Aza na, "Ultrafast spectrogram with sub-THz bandwidth," in *2022 IEEE Photonics Conference (IPC)*, (IEEE, 2022), pp. 1–2.
26. O. Kuzucu, F. N. Wong, S. Kurimura, *et al.*, "Time-resolved single-photon detection by femtosecond upconversion," Opt. Lett. **33**(19), 2257–2259 (2008).
27. S. J. Soundararajan, L. Yang, S. Zhang, *et al.*, "Time-wavelength optical sampling spectroscopy based on dynamic laser cavity tuning," J. Opt. Soc. Am. B **35**(5), 1186–1191 (2018).
28. S. J. Soundararajan and L. Duan, "Time-stretch spectroscopy based on laser cavity tuning with a dual-function delay line," IEEE Photonics Technol. Lett. **31**(16), 1385–1388 (2019).

Optics EXPRESS

29. S. J. Soundararajan and L. Duan, "Real-time TWOS spectroscopy with sub-GHz resolution and high sensitivity," Opt. Express **29**(25), 41512–41521 (2021).
30. T. Hochrein, R. Wilk, M. Mei, *et al.*, "Optical sampling by laser cavity tuning," Opt. Express **18**(2), 1613–1617 (2010).
31. L. Yang, J. Nie, and L. Duan, "Dynamic optical sampling by cavity tuning and its application in lidar," Opt. Express **21**(3), 3850–3860 (2013).
32. Y. Cai, Y. Chen, K. Dorfman, *et al.*, "Mid-infrared single-photon upconversion spectroscopy enabled by nonlocal wavelength-to-time mapping," Sci. Adv. **10**(16), eadl3503 (2024).
33. K. L. Fenwick, D. G. England, P. J. Bustard, *et al.*, "Carving out configurable ultrafast pulses from a continuous wave source via the optical Kerr effect," Opt. Express **28**(17), 24845–24853 (2020).
34. A. R. Cameron, K. L. Fenwick, S. W. Cheng, *et al.*, "Ultrafast measurement of energy-time entanglement with an optical Kerr shutter," Phys. Rev. A **108**(4), L041503 (2023).
35. F. Bouchard, D. England, P. J. Bustard, *et al.*, "Achieving ultimate noise tolerance in quantum communication," Phys. Rev. Appl. **15**(2), 024027 (2021).
36. K. L. Fenwick, F. Bouchard, G. S. Thekkadath, *et al.*, "Photonic quantum walk with ultrafast time-bin encoding," Optica **11**(7), 1017–1023 (2024).
37. F. Bouchard, K. Fenwick, K. Bonsma-Fisher, *et al.*, "Programmable photonic quantum circuits with ultrafast time-bin encoding," Phys. Rev. Lett. **133**(9), 090601 (2024).
38. A. M. Weiner, *Ultrafast optics* (John Wiley & Sons, 2011).
39. L. Lepetit, G. Chériaux, and M. Joffre, "Linear techniques of phase measurement by femtosecond spectral interferometry for applications in spectroscopy," J. Opt. Soc. Am. B **12**(12), 2467–2474 (1995).
40. Schott, "TIE-31: Mechanical and thermal properties of optical glass," (2010).
41. D. England, F. Bouchard, K. Fenwick, *et al.*, "Perspectives on all-optical Kerr switching for quantum optical applications," Appl. Phys. Lett. **119**(16), 160501 (2021).
42. C. Kupchak, J. Erskine, D. England, *et al.*, "Terahertz-bandwidth switching of heralded single photons," Opt. Lett. **44**(6), 1427–1430 (2019).
43. C. Kupchak, P. J. Bustard, K. Heshami, *et al.*, "Time-bin-to-polarization conversion of ultrafast photonic qubits," Phys. Rev. A **96**(5), 053812 (2017).
44. S. Arzhantsev and M. Maroncelli, "Design and characterization of a femtosecond fluorescence spectrometer based on optical Kerr gating," Appl. Spectrosc. **59**(2), 206–220 (2005).
45. S. Arzhantsev, H. Jin, G. A. Baker, *et al.*, "Measurements of the complete solvation response in ionic liquids," J. Phys. Chem. B **111**(18), 4978–4989 (2007).
46. S. Kinoshita, H. Ozawa, Y. Kanematsu, *et al.*, "Efficient optical Kerr shutter for femtosecond time-resolved luminescence spectroscopy," Rev. Sci. Instrum. **71**(9), 3317–3322 (2000).
47. J. Takeda, K. Nakajima, S. Kurita, *et al.*, "Time-resolved luminescence spectroscopy by the optical Kerr-gate method applicable to ultrafast relaxation processes," Phys. Rev. B **62**(15), 10083–10087 (2000).
48. B. Schmidt, S. Laimgruber, W. Zinth, *et al.*, "A broadband Kerr shutter for femtosecond fluorescence spectroscopy," Appl. Phys. B **76**(8), 809–814 (2003).
49. I. A. Walmsley and C. Dorrer, "Characterization of ultrashort electromagnetic pulses," Adv. Opt. Photonics **1**(2), 308–437 (2009).